Nuclear Instruments and Methods in Physics Research A 352 (1995) 583–587

NUCLEAR INSTRUMENTS & METHODS IN PHYSICS RESEARCH Section A

ELSEVIER

Nuclear spectroscopy using lasers at Oak Ridge National Laboratory: experiments with stable (past) and radioactive (future) tandem beams

H.A. Schuessler [a,d,*], E.C. Benck [a], F. Buchinger [b], H.K. Carter [c]

[a] *Department of Physics, Texas A&M University, College Station, TX 77843, USA*
[b] *Foster Radiation Laboratory, McGill University, Montreal, Canada H3A8B*
[c] *UNISOR, Oak Ridge, Associated Universities, Oak Ridge, TN 37831, USA*
[d] *Institute for Nuclear Study, University of Tokyo, Tanashi, Tokyo 188, Japan*

Received 6 July 1994

Abstract

Fast beam collinear laser spectroscopy has yielded information on nuclear structure on the long chain of neutron deficient Tl isotopes ($186 \leq A \leq 205$) using heavy ion fusion evaporation reactions to produce Tl-ion beams which for the most neutron deficient isotope were only about 10^4/s. The new radioactive heavy ion beam facility projected to be completed in 1995 requires even higher sensitivities at the few 10 nuclei/s level. Two examples to realize such ultra-sensitive measurements employing laser techniques are described. They are: field-ionization spectroscopy in a fast beam and stored ion spectroscopy in a novel linear combined trap.

1. Introduction

The first part of this paper summarizes the laser spectroscopy measurements performed at Oak Ridge National Laboratory (ORNL) on the long chain of thallium isotopes ($186 \leq A \leq 205$). In it the results and a short discussion of our most recent measurement namely of ^{186}Tl are included. The second part is concerned with reporting on our efforts to adapt collinear fast beam laser spectroscopy to the minute yields expected at the Holifield Radioactive Ion-Beam Facility (HRIBF). In addition a novel trapping device, the linear combined trap is illustrated and will also be used there.

2. Summary of the nuclear moments and isotope shift measurements of Tl

The laser spectroscopy measurements on the thallium isotopes ($Z = 81$) reaches on the neutron deficient side to ^{186}Tl ($N = 105$) starting at the valley of stability at ^{205}Tl ($N = 124$) which is close to a neutron shell closure. The isotopes include ground and isomeric states with nuclear spins of $I = 1/2$, $9/2$ and 7. The nuclear moments and charge radii have previously been reported in detail [1–5] with the exception of ^{186}Tl. Table 1 summarizes our recent results for ^{186}Tl. For this isotope the configuration is $\pi s_{1/2} \times \nu i_{13/2}$ with the nuclear spin given by $I = j_1 + j_2 = 7$. In this case the magnetic moment can also be found as the sum of moments of the one particle configurations as $\mu = 0.51\mu_N$. This value is in good agreement with the experimentally derived value of $\mu = 0.497(9)\mu_N$, which was obtained from the ratio of the measured A factors according to

$$\mu_{186} = (A_{186}/A_{205})(I_{186}/I_{205})\mu_{205}. \quad (1)$$

Here we neglect the small contribution of about 6×10^{-3} due to the hyperfine structure anomaly. The nuclear moment compares also well with another way of estimating its expected value, namely by combining the measured values of the magnetic moments of the $I = 1/2$ state of ^{187}Tl ($\mu = 1.55(6)\mu_N$) and of the $I = 13/2$ state of the ^{185}Hg isotone ($\mu = -1.07(7)\mu_N$) which have the same proton or neutron configurations respectively as ^{186}Tl. Fig. 1 summarizes the results for all Tl isotopes and indicates that for each configuration the magnetic moment does not change significantly with neutron number.

Table 1
Isotope shift relative to ^{205}Tl and HFS parameters in the $\lambda = 535$ nm line

Isotope	IS^{186,205} (GHz)	A ($7s\ ^2S_{1/2}$) (MHz)	A ($6p\ ^2P_{3/2}$) (MHz)	B ($6p\ ^2P_{3/2}$) (MHz)
186	−15.895(25)	265.6(6)	2.4(3.0)	−70(6)

* Corresponding author. Tel. +1 409 845 7717, Fax +1 409 845 2590.

SSDI 0168-9002(94)00889-2

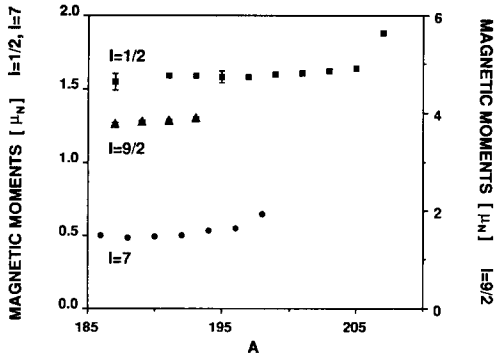

Fig. 1. Magnetic moments of the $I = 1/2$, $I = 9/2$, and $I = 7$ states of the neutron-deficient Tl isotopes.

For the extraction of the spectroscopic quadrupole moment Q_s of ^{186}Tl from the measured B factor, we use the relation of Rosen and Lindgren [6] $Q_s = (8.9 \times 10^{-4}$ b/MHz)B without including a Sternheimer correction. The value for ^{186}Tl is $Q_s = 0.06(10)$ b. This results together with the values of Q_s of the other $I = 7$ isomers are plotted in Fig. 2. The spectroscopic quadrupole moments show a linear decrease with decreasing mass number. A linear dependence of the moments with mass number is expected in an independent particle approach, where the moment depends on the occupation number of a subshell (n) as

$$Q = Q_{sp}[(2j + 1 - 2n)/(2j - 1)]. \quad (2)$$

Here, Q_{sp} is the single-particle quadrupole moment for the $1i_{13/2}$ orbital and $j = 13/2$ since in a pure $\pi s_{1/2} \nu i_{13/2}$ shell model configuration the proton contribution to the moment vanishes. A change in sign near the middle of the subshell is indicated. Since the quadrupole moment is mainly generated from the $1i_{13/2}$ neutron orbital, the variation in Q_s for the $I = 13/2^+$ isomers in the neighboring Hg should be very much the same as for the 7^+ state in the odd–odd Tl nuclei. This is indeed the case, as is shown in the figure. Thus, the variation for both the Hg and Tl nuclei, as a function of neutron number, reflects mainly the occupancy of the neutron $1i_{13/2}$ single-particle orbital as indicated by Eq. (2). The quadrupole moments of the $I = 9/2$ isotopes have also been reported [2–5] and reference is made to that work.

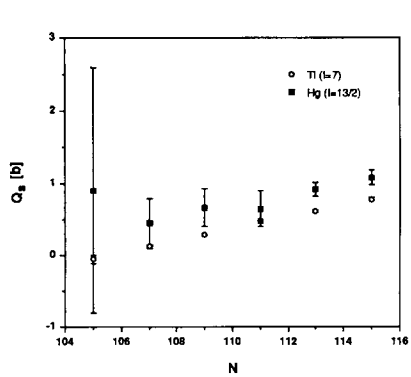

Fig. 2. Spectroscopic quadrupole moments of the $I = 7$ isomers of Tl and the $I = 13/2$ isomers of Hg [1]. Where not shown, the uncertainty is less than the size of the symbol.

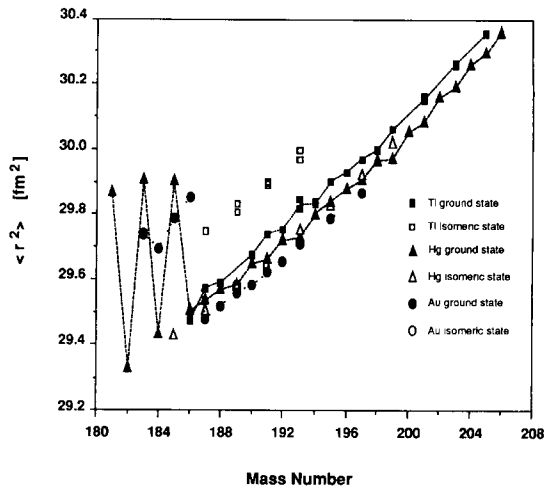

Fig. 3. Mean-square charge radii of thallium, gold and mercury isotopes as a function of mass-number. The radii of the ground states are indicated and connected by an eye-guiding line. In addition the charge radii of isomeric states are given.

It is well known that for the transitional nuclei near the closed proton shell at $Z = 82$ shape isomerism occurs. This can be studied in a systematic way when reducing the neutron number. A sudden drastic change in the isotope shift indicating shape isomerism was first observed [7] for mercury between the ^{185}Hg and ^{187}Hg ($N = 105$ and 107) isotopes and is the due to the near degeneracy of the nuclear states of different nuclear shape. Subsequently a similar behavior was measured [8] for the nearby Au-isotopes between ^{186}Au and ^{187}Au ($N = 107$ and 108). It is therefore interesting to find out whether in thallium for ^{186}Tl ($N = 105$) such a shape transition already takes place. The isotope shift of ^{186}Tl is listed in Table 1 and indicates that for Tl such a transition has not yet occurred down to $N \geq 105$. Fig. 3 illustrates this situation and displays the mean square charge radii of the various Tl isotopes versus N and compares them to the corresponding values of Au and Hg.

3. Preparation of laser spectroscopy experiments at the HRIBF

Fig. 4 displays a section of the chart of nuclei near the proton drip line for $Z = 36$–38 nuclei. Such nuclei will be produced at HRIBF and have been selected for their physics interest. On the dashed line lie the nuclei with $Z = N$. Our initial project is to study the optical isotope

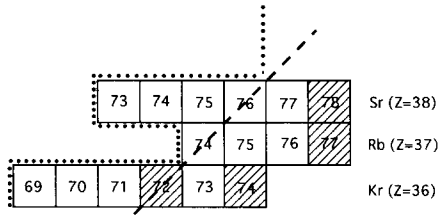

Fig. 4. Section of the chart of nuclei near the proton drip line for $Z = 36$–38 nuclei. On the dashed line lie the nuclei with $Z = N$. Open squares indicate nuclei which have not been studied. Nuclei to the left of the dotted line are predicted to be particle unstable by the mass model of Janecke and Masson.

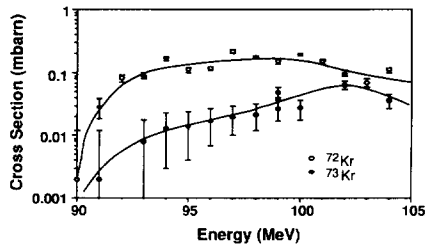

Fig. 5. Cross sections versus the heavy ion beam energy for the $^{40}Ca(^{34}Cl,pxn)^{73-x}Kr$ heavy ion fusion-evaporation reaction. The solid lines were drawn to guide the eye.

shifts and hyperfine structure of these very neutron deficient krypton isotopes near the proton drip line. Of particular interest is the region $N = Z = 36$ where the onset of large deformations as well as shape coexistence in the same nucleus are predicted. Our measurement technique applies with minor modifications also to Rb ($Z = 37$) and Sr ($Z = 38$). We propose therefore to study the development of the deformed magic number at $Z = N = 38$ and the oblate–prolate shape competition in the region of neutron deficient isotopes of elements with $Z = 36$–38. The large deformations of the nuclear ground states in this region are due to the reinforcing of the proton and neutron shape driving forces associated with the shell gaps at the large deformation of $\beta = 0.4$.

An additional result of the proposed measurement is to extend the measurements of the odd–even staggering parameter for the neutron deficient krypton, rubidium, and strontium isotopes towards smaller N. There is a sign change in this parameter for nuclei with $N \leq 43$. The ground states of the odd–even nuclei could correspond to completely different core states, since in this region there are many minima in the total potential energy for different deformation values.

We also propose to perform hyperfine structure measurements at the HRIBF of the light indium nuclei using the $\lambda = 231$ nm optical line. The isotopes having masses 99–104 will be produced to determine their nuclear radii and nuclear moments. In particular the nuclear magnetic moments of the odd–odd nuclei are of interest to study neutron configuration admixtures.

We are presently investigating yields of possible target materials to be used with the projected initial beams of the HRIBF through the use of the PACE2 code. The calculated heavy ion fusion evaporation reaction cross sections of krypton isotopes close to the proton drip line are given in Fig. 5. For a primary ^{34}Cl beam of 10^{10} particles/s the yields will be at or below the 100 nuclei per second range

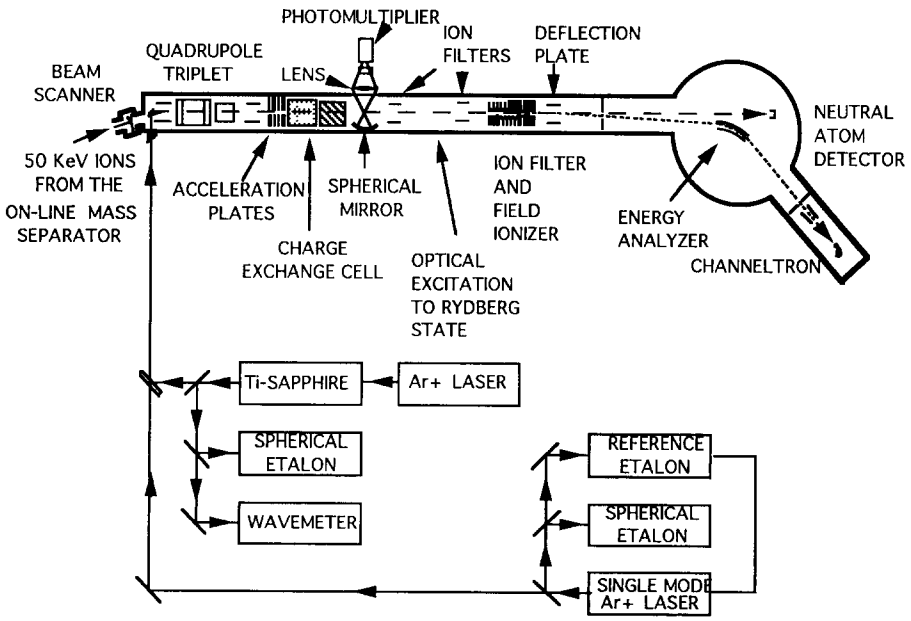

Fig. 6. Experimental apparatus for collinear fast beam laser spectroscopy using two step excitation and field ionization with charged particle detection.

with a large isobaric background. Therefore a highly sensitive and selective detection scheme is required for their study. The recoil ions from the HRIBF target will be stopped in a foil, desorbed, and ionized by a pulsed laser. Alternatively an on-line ion source will be used.

3.1. Two-photon stepwise-laser excitation and field-ionization in a collinear beam

Our present on-line collinear fast beam apparatus is being improved to include particle detection after two-photon stepwise-laser excitation followed by field ionization. This detection scheme monitors all ions which have been resonantly excited and is not limited by the finite solid angle of optical detection. It therefore combines the high efficiency of charged particle detection with the high selectivity of photon excitation. A sensitivity of a few 10 nuclei/s and a selectivity of better than 1 nucleus in 10^{10} nuclei from neighboring isotopes is predicted.

The first step in our detection scheme is to convert the fast krypton ion beam emerging from the on-line mass separator or the target area into a fast metastable krypton atom beam. This is accomplished through a near-resonant charge exchange collision reaction with an alkali metal vapor. The metastable krypton atoms are then optically excited through a resonant intermediate level into a Rydberg state using two laser wavelengths of $\lambda = 811$ and $\lambda = 488$ nm. Both lasers are collinear with the fast atom beam, so that Doppler-free spectral line widths are obtained through velocity bunching. The Rydberg atoms are subsequently ionized by an axial electric field at a particular electric potential. This energy labels the resulting ion beam so that background ionization events can be discriminated against with an energy analyzer. Single krypton ions are finally counted with a channeltron.

A test apparatus has been constructed at Texas A&M University to optimize this detection scheme using stable krypton isotopes and is depicted in Fig. 6. It uses a single mode Ti–sapphire and Ar^+ lasers for excitation and an optimized field ionization region [9].

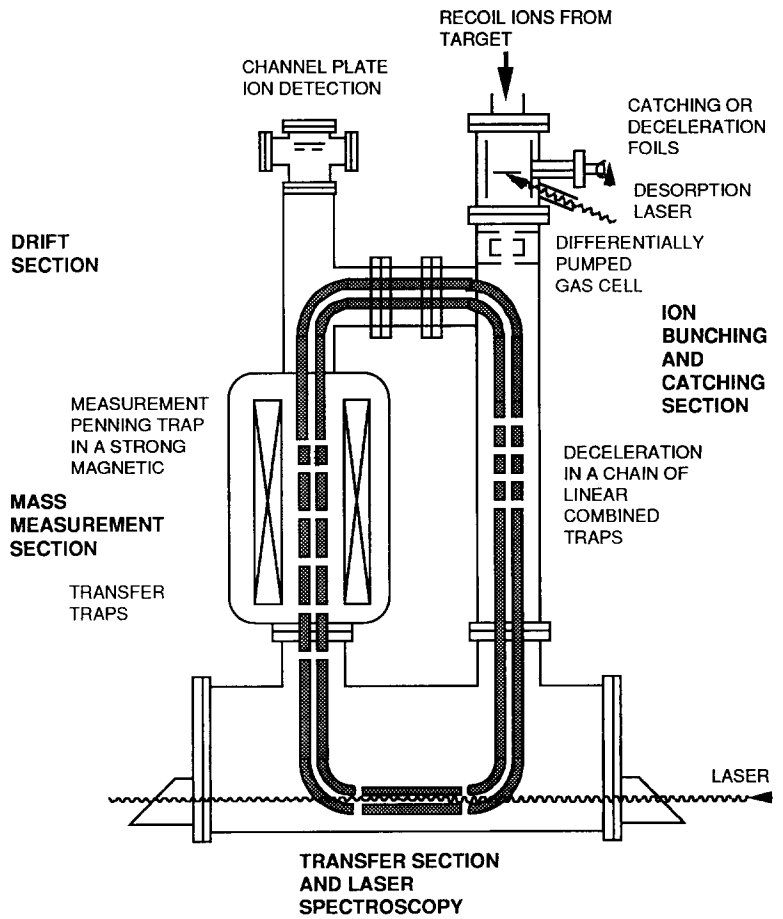

Fig. 7. Proposed linear combined trap for the HRIBF-facility.

3.2. Laser spectroscopy with a linear combined trap

We have developed and tested a prototype linear combined trap [10]. This device promises to have the capability to measure at the single nucleus level. Its basic structure is that of a racetrack with a circumference of 56 cm. It was developed to facilitate ion storage, laser spectroscopy, and possibly laser cooling in the straight sections. The trapping device can also be used to study other ions, such as Sr^+ and Tl^+. Fig. 7 shows schematically its construction.

The trap arrangement is split into several sections and the structure is closed upon itself allowing the ions to circulate in the trap and repeatedly interact with the various manipulation fields and the laser beam. By properly biasing the trap segments, ions can be transported to accumulate and reside in any region of the racetrack arrangement. Also any section can be operated as a combined trap, a Paul RF trap, or a Penning magnetic field trap. The advantage of the linear trap over conventional Paul and Penning traps is that the potential valley along the axis allows the storage of many ions simultaneously in the field free region of the trap valley. This improves the signal to noise ratios for laser cooled ion trap experiments.

Our general trapping device has the advantage of allowing repeated collinear beam spectroscopy on the stored ions, Doppler free spectroscopy, laser cooling, and single ion detection.

We propose three injection schemes of increasing efficiency and complexity:

- foil implantation of the short lived ions followed by laser ablation and ionization at the edge of the trap;
- energy degradation of the short-lived ions by stopping foils and decelerating pulses;
- use of an electric ion guide [11] and a differentially pumped stopping gas at the injection site.

We have performed initial measurements with a segmented-linear ion trap to test the new trap design. Measurements with a racetrack-trap are beginning. Injection, transfer, and storage of charged particles have been done. In addition the laser desorption process is being studied by detecting the ions generated, and by simultaneously also monitoring the optical fluorescence of the desorbed material.

4. Conclusion

The study of the new nuclei which will become available at the HRIBF requires the development of novel ultra sensitive detection instrumentation. We have given two examples of how to proceed: field ionization with energy labeling in a beam, and particle storage in an ion trap. In particular the on-line combined trap, once fully developed, will rival a recoil mass separator and can be built at a fraction of its cost. The on-line combined trap should find applications in both nuclear and optical spectroscopy experiments.

Acknowledgement

This work is supported by DOE and a Teledyne Research Assistance grant.

References

[1] E.W. Otten in: Treatise on Heavy Ion Science, Vol. 8, ed. A. Bromley (Plenum, New York, 1989).
[2] J.A. Bounds, C.R. Bingham, H.K. Carter, G.A. Leander, R.L. Mlekodaj, E.H. Spejewski and W.M. Fairbank, Jr., Phys. Rev. C 36 (1987) 2560.
[3] H.A. Schuessler, E.C. Benck, F. Buchinger, H. Iimura, Y.F. Li, C. Bingham and H.K. Carter, Hyperfine Interactions 74 (1992) 13.
[4] F. Buchinger, H.A. Schuessler, E.C. Benck, H. Iimura, Y.F. Li, C. Bingham and H.K. Carter, Hyperfine Interactions 75 (1992) 367.
[5] R. Menges, U. Dinger, N. Boos, G. Huber, S. Schröder, S. Dutta, R. Kirchner, O. Klepper, T. Kuhl, D. Marx and G.D. Sprouse, Z. Phys. A 341 (1992) 475.
[6] I. Lindgren and A. Rosen, Case Studies At. Coll. Phys. 453 (1975).
[7] J. Bonn, G. Huber, H.J. Kluge and E. Otten, Z. Phys. A 276 (1976) 203.
[8] K. Wallmeroth, G. Bollen, A. Hohn, P. Engelhof, J. Gruener, F. Lindenlauf, U. Kroenert, J. Campos, A. Yunta, M. Borge, J. Wood, R. Moore and H.J. Kluge, Phys. Rev. Lett. 58 (1987) 1516.
[9] Kay Stratmann, Diplomarbeit, Johannes-Gutenberg-Universität Mainz (1991).
[10] H.A. Schuessler, E.C. Benck and J. Lassen, Hyperfine Interactions 81 (1993) 263.
[11] H.J. Xu, M. Wada, J. Tanaka, H. Kawami and I. Katayama, Nucl. Instr. and Meth. A 333 (1993) 274.